

Supporting Information for ”Sea surface temperature control on the aerosol-induced brightness of marine clouds over the North Atlantic Ocean”

Xiaoli Zhou^{1,2}, Jianhao Zhang^{1,3}, Graham Feingold^{1,2}

¹Chemical Sciences Laboratory, NOAA, Boulder, Colorado, USA

²Cooperative Institute for Research in Environmental Sciences (CIRES), University of Colorado, Boulder, Colorado, USA

³National Academies/National Research Council (NRC) Fellowship

Contents of this file

1. Text S1
2. Figures S1 to S9

Text S1: Influence of precipitation on aerosol-induced cloud albedo susceptibility

To investigate the influence of precipitation on aerosol-induced cloud albedo susceptibility (S_0), we quantify the rain rate (RR) reduction susceptibility to changes in cloud droplet number concentration (N_d) at fixed RR bins (Fig. S1) following (Sorooshian et al., 2009). Fig. S1 shows that the RR reduction susceptibility increases with RR for $RR \leq 0.4$ mm day⁻¹ where aerosol effectively suppress precipitation. For $RR > 0.4$ mm day⁻¹, the

susceptibility begins to slightly decrease because the precipitation process becomes relatively efficient such that the aerosol-induced cloud water adjustment is more than offset by the precipitation removal of cloud water. However, the relatively high rain rate occurs less than 20% of the time over the North Atlantic (Fig. S1)), so we do not expect a strong influence of it on S_0 . In fact, S_0 barely changes if relatively heavy precipitation cases ($RR > 0.3 \text{ mm day}^{-1}$) are excluded (Fig. S2). This suggests that precipitation scavenging does not play a critical role in generating darkening clouds over the North Atlantic.

References

- Sorooshian, A., Feingold, G., Lebsock, M. D., Jiang, H., & Stephens, G. L. (2009). On the precipitation susceptibility of clouds to aerosol perturbations. *Geophysical Research Letters*, *36*(13).

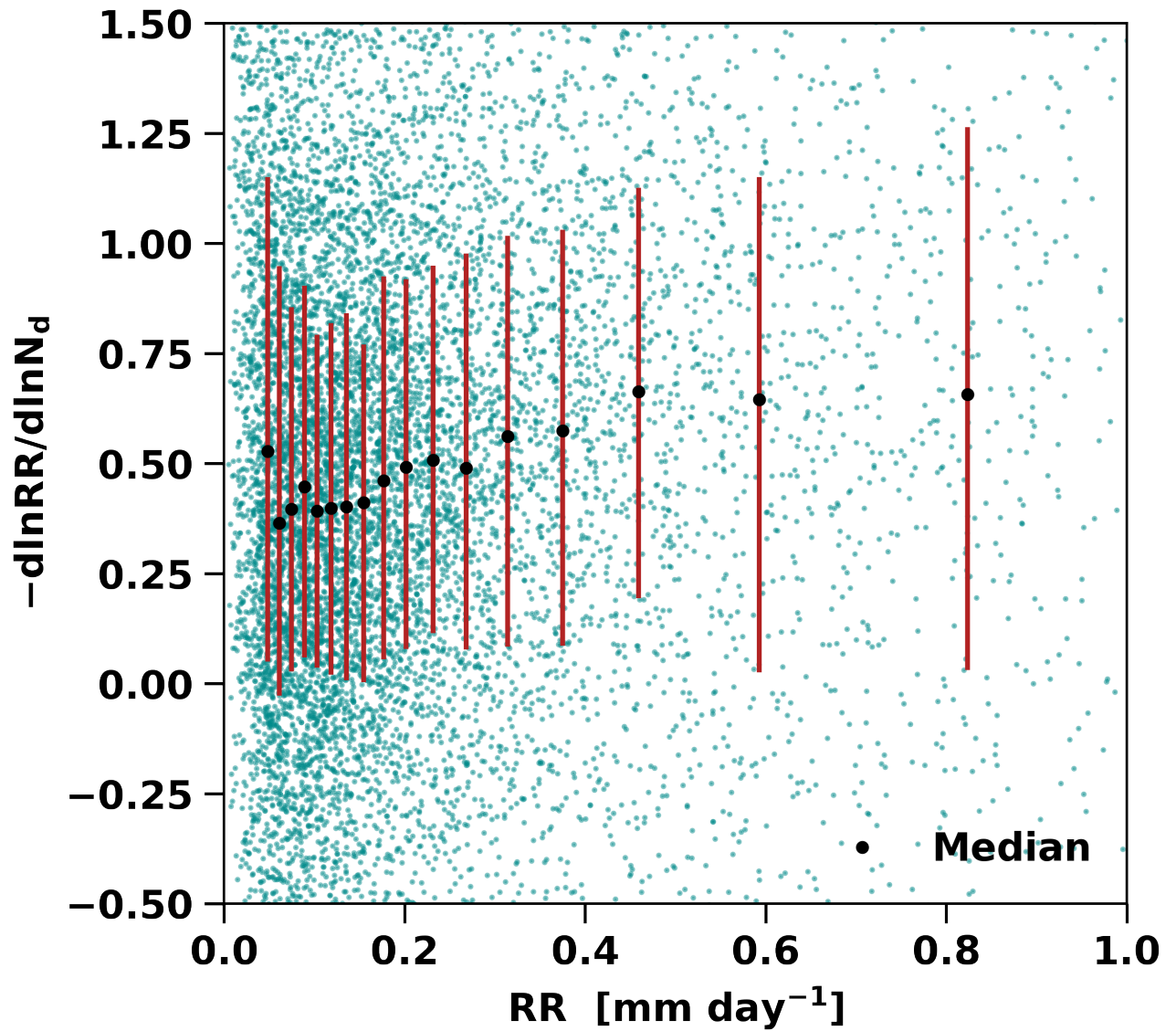


Figure S1. Scatter plot (green dots) of rain rate (RR) and RR reduction susceptibility to cloud droplet number concentration (N_d) perturbations, overlaid by median (black dot), and interquartile range (red vertical line) of RR reduction susceptibility in each RR bin (5%).

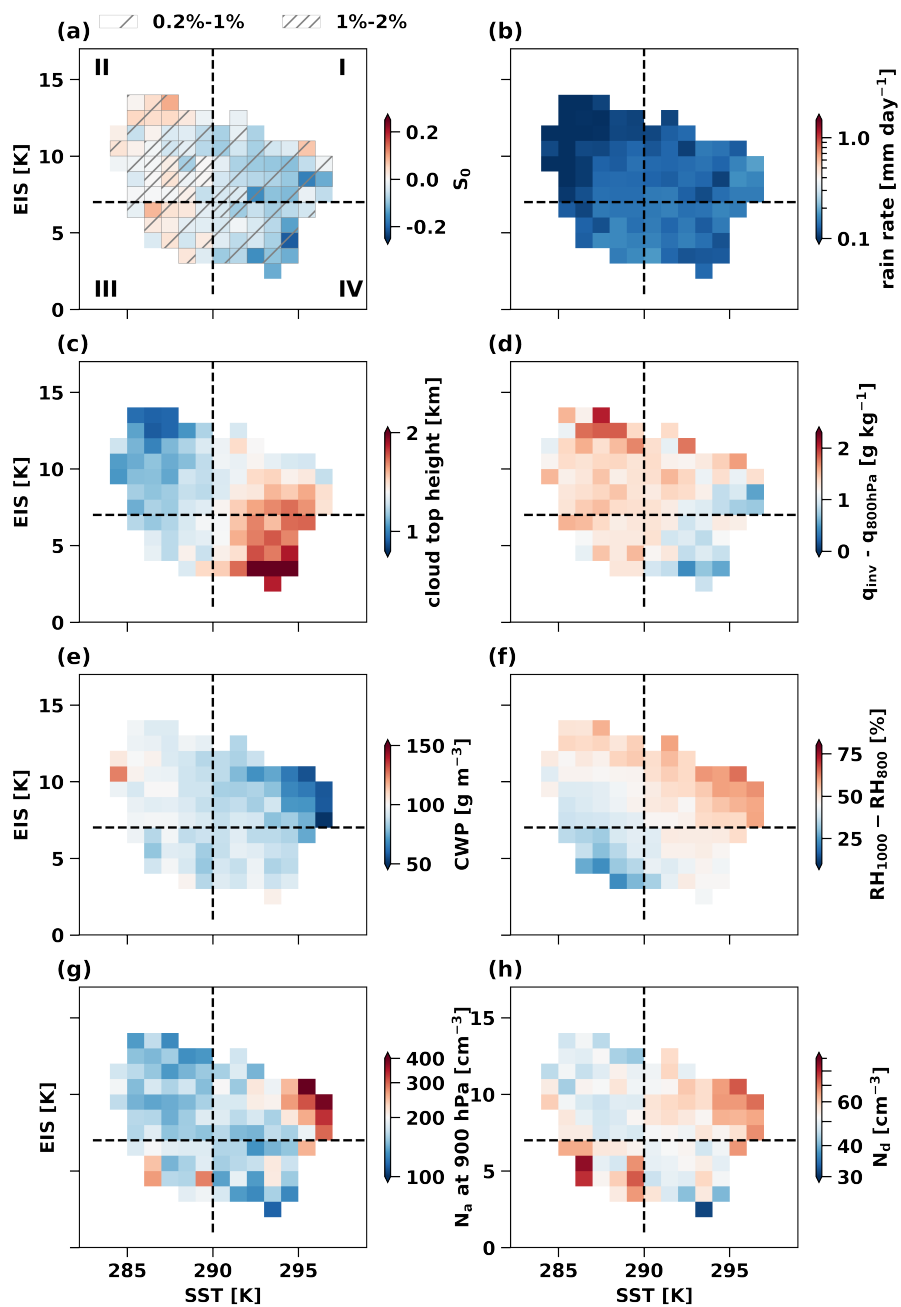


Figure S2. Same as Fig. 2 but for rain rate less than 0.3 mm day⁻¹.

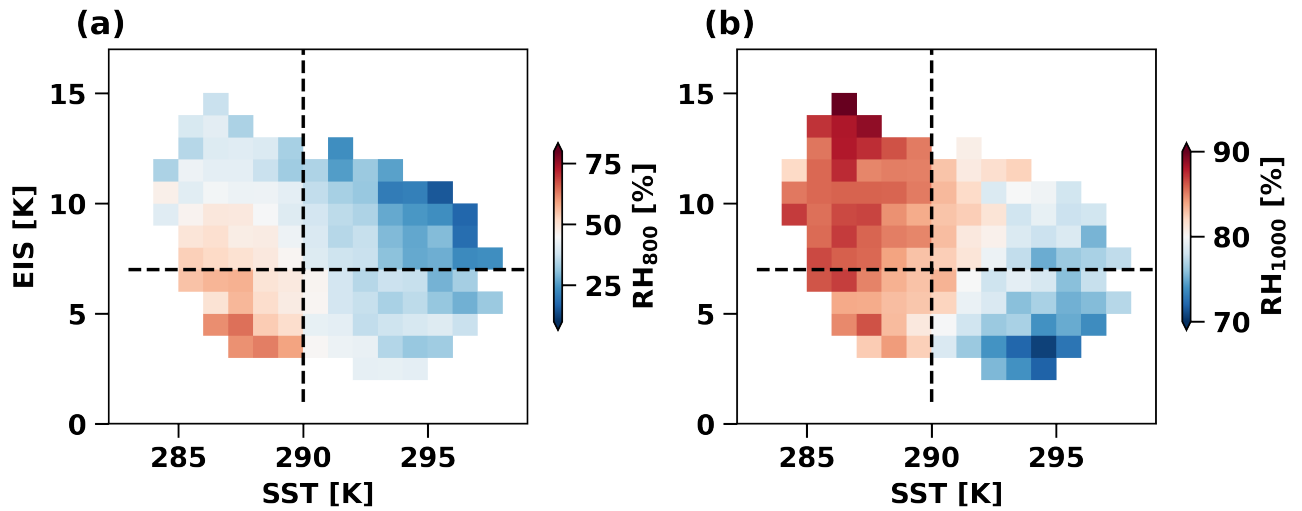


Figure S3. The mean values of (a) relative humidity at 800 hPa (RH_{800}) and (b) relative humidity at 1000 hPa (RH_{1000}) within bins of estimated inversion strength and sea surface temperature. The bin width is 1K Δ EIS in the vertical and 5K Δ SST in the horizontal. At least 20 samples are required in each bin. Black dashes indicate SST = 290 K and EIS = 7 K isolines.

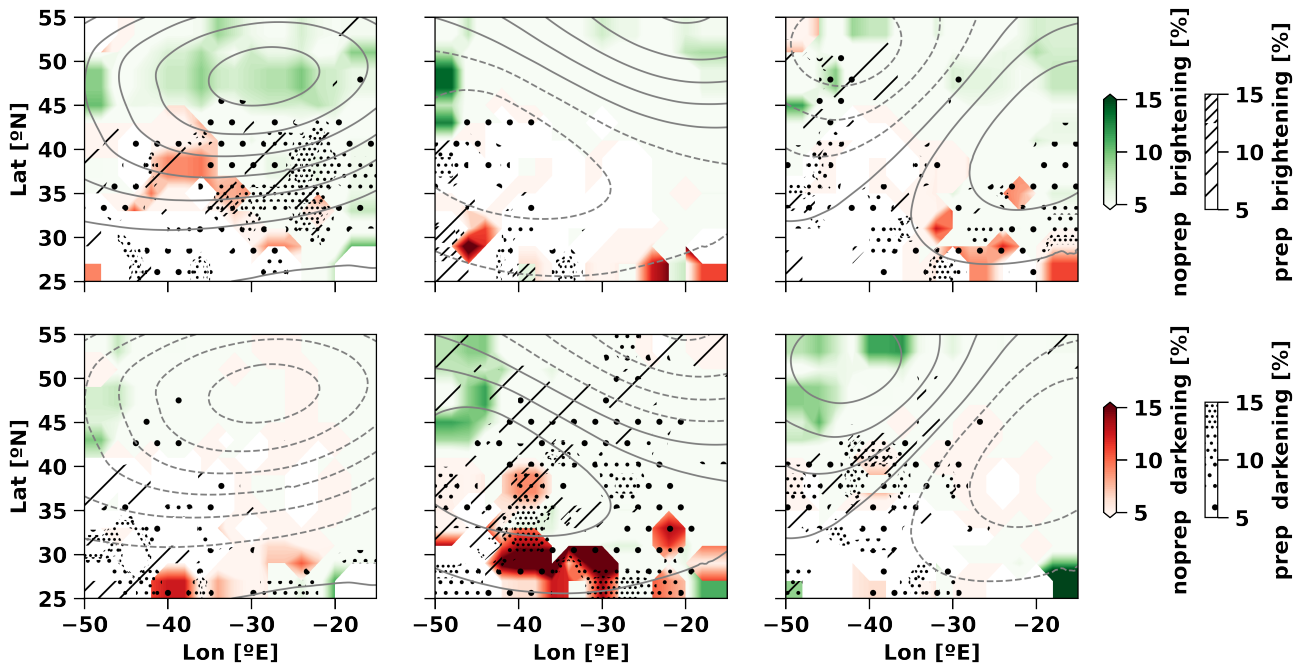


Figure S4. Frequency of occurrence for nonprecipitating brightening clouds (rain rate ≤ 0.24 mm day $^{-1}$ and the cloud albedo susceptibility to cloud droplet number concentration perturbations $S_0 > 0$, green shading), nonprecipitating darkening clouds (rain rate ≤ 0.24 mm day $^{-1}$ and $S_0 < 0$, red shading), precipitating brightening clouds (rain rate > 0.24 mm day $^{-1}$ and $S_0 > 0$, hatches), and precipitating darkening clouds (rain rate > 0.24 mm day $^{-1}$ and $S_0 < 0$, dots) in the first three modes of the Empirical Orthogonal Function Analysis of surface pressure perturbations. The patterns in the second row are identical to that in the first row but with flipped sign.

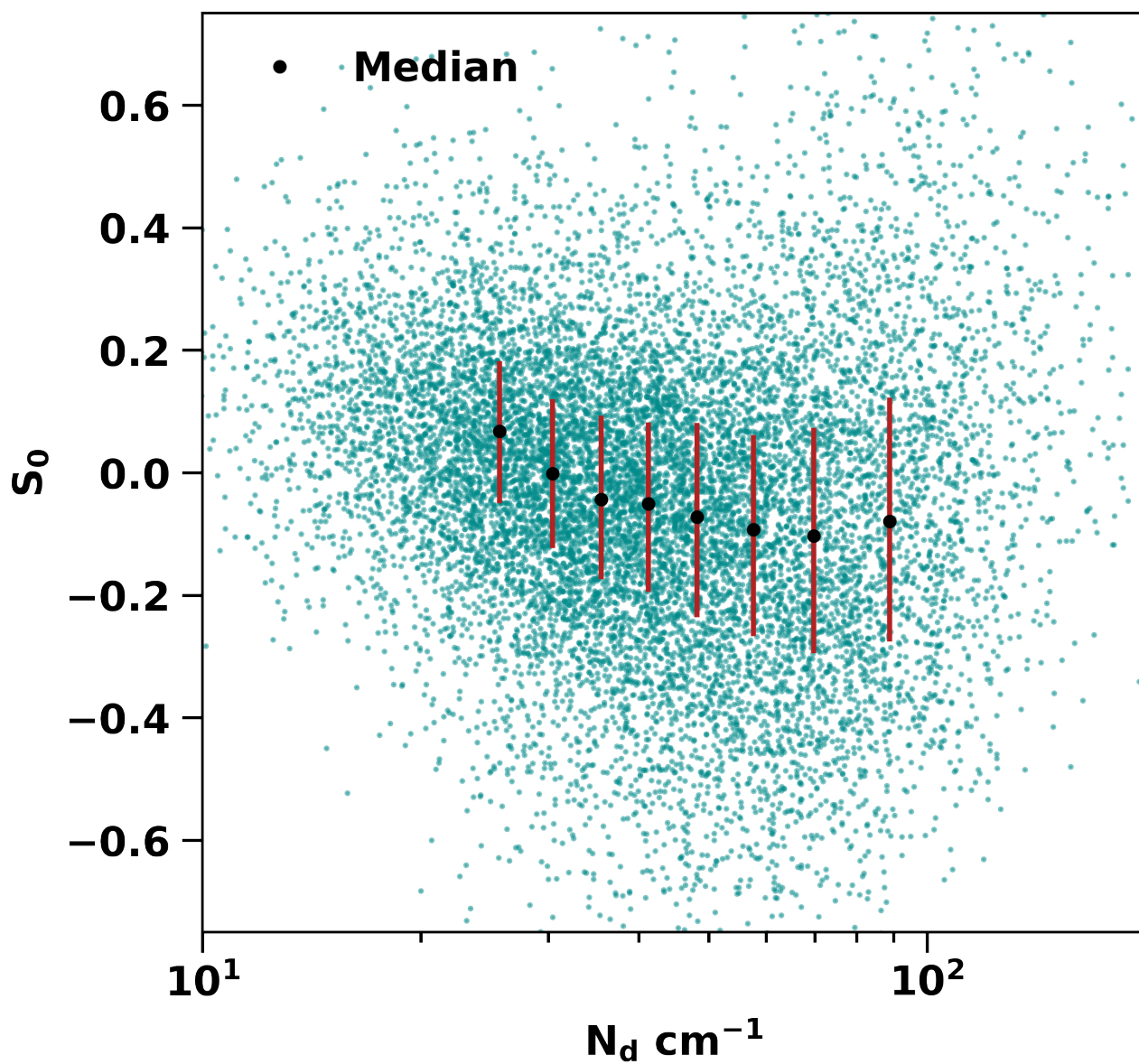


Figure S5. Scatter plot (green dots) of cloud droplet number concentration (N_d) and cloud albedo susceptibility to N_d perturbations (S_0), overlaid by median (black dot) and interquartile range in each N_d bin (10%).

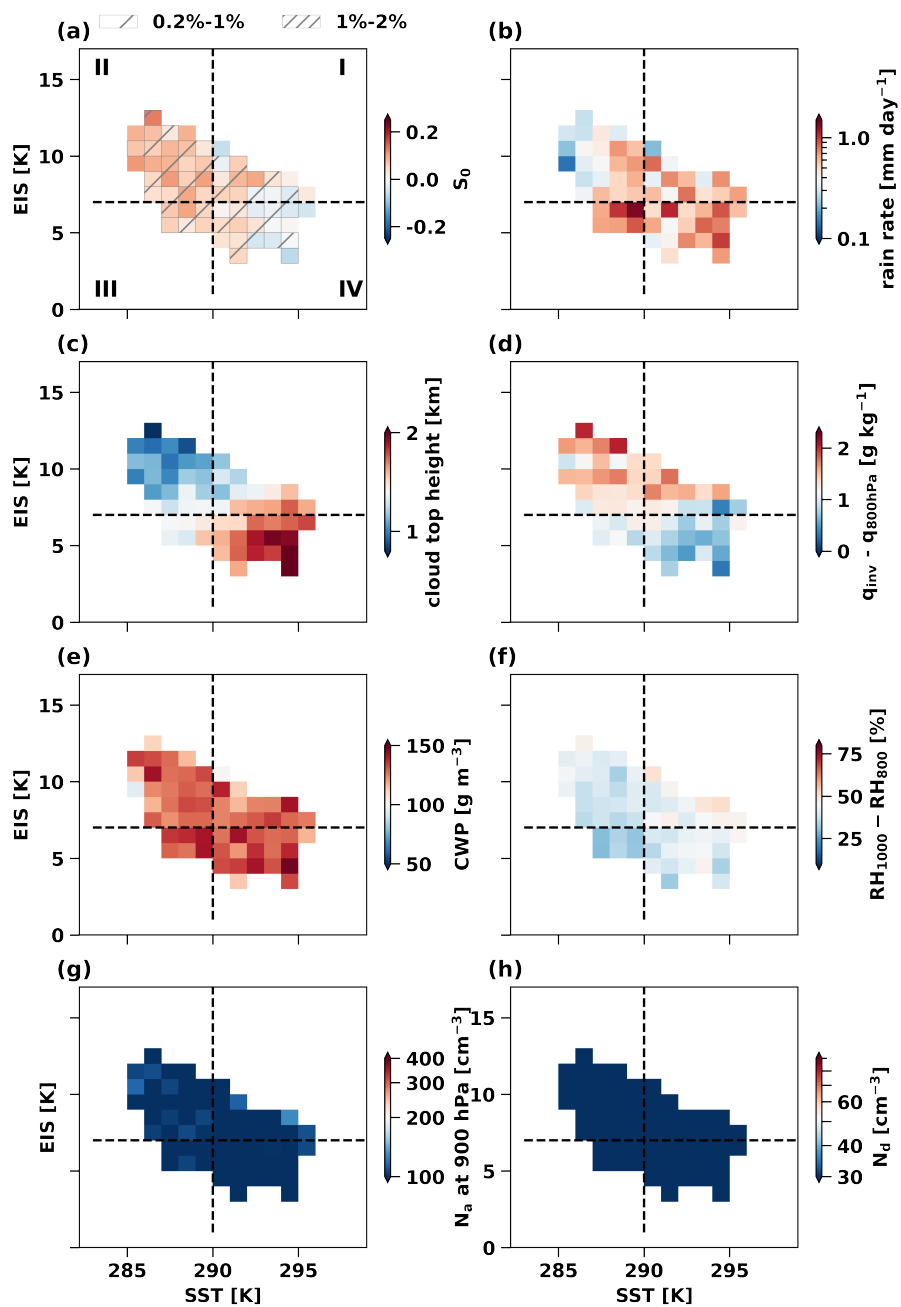


Figure S6. Same as Fig. 2 but for $N_d < 30\text{cm}^{-3}$.

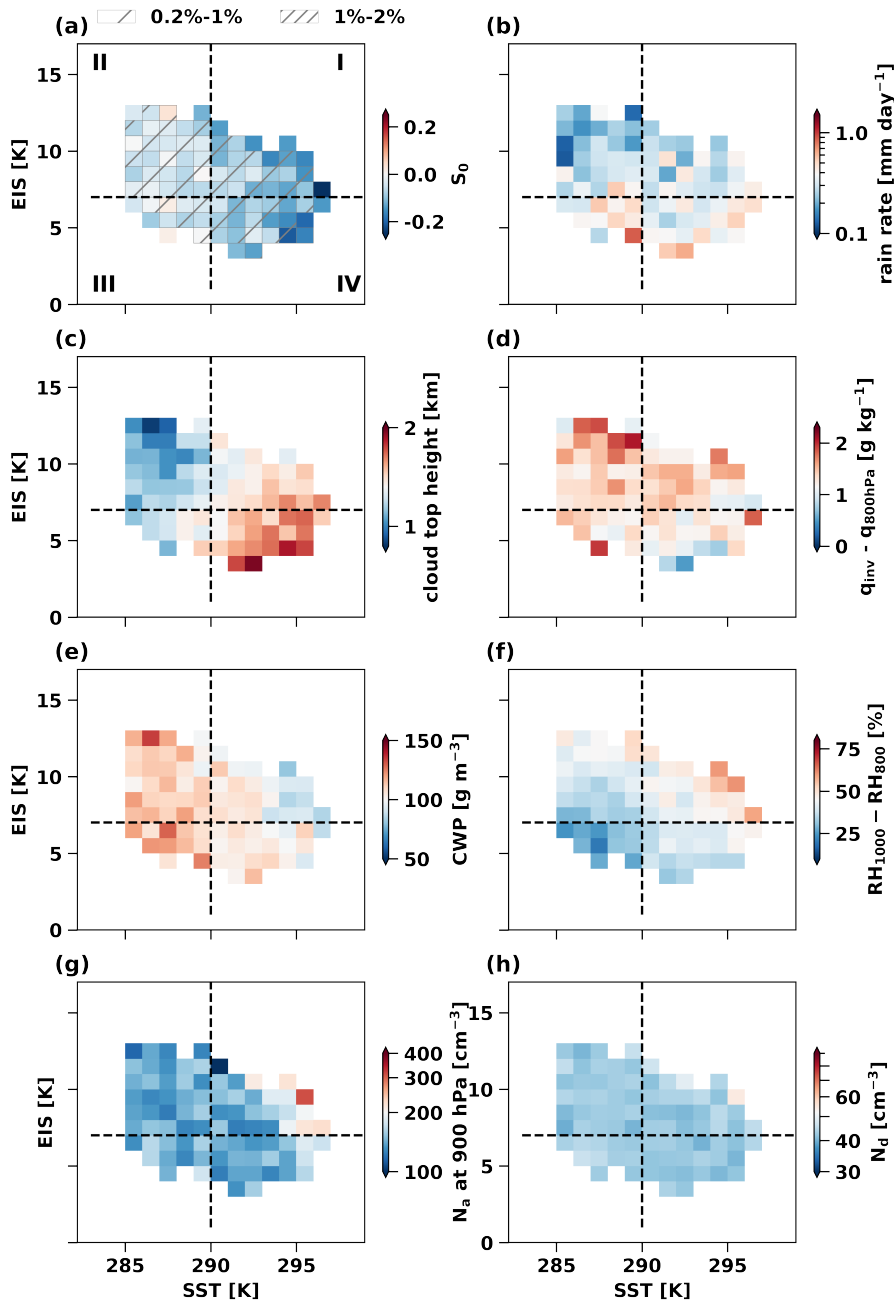


Figure S7. Same as Fig. 2 but for $30 \leq N_d < 60 \text{ cm}^{-3}$.

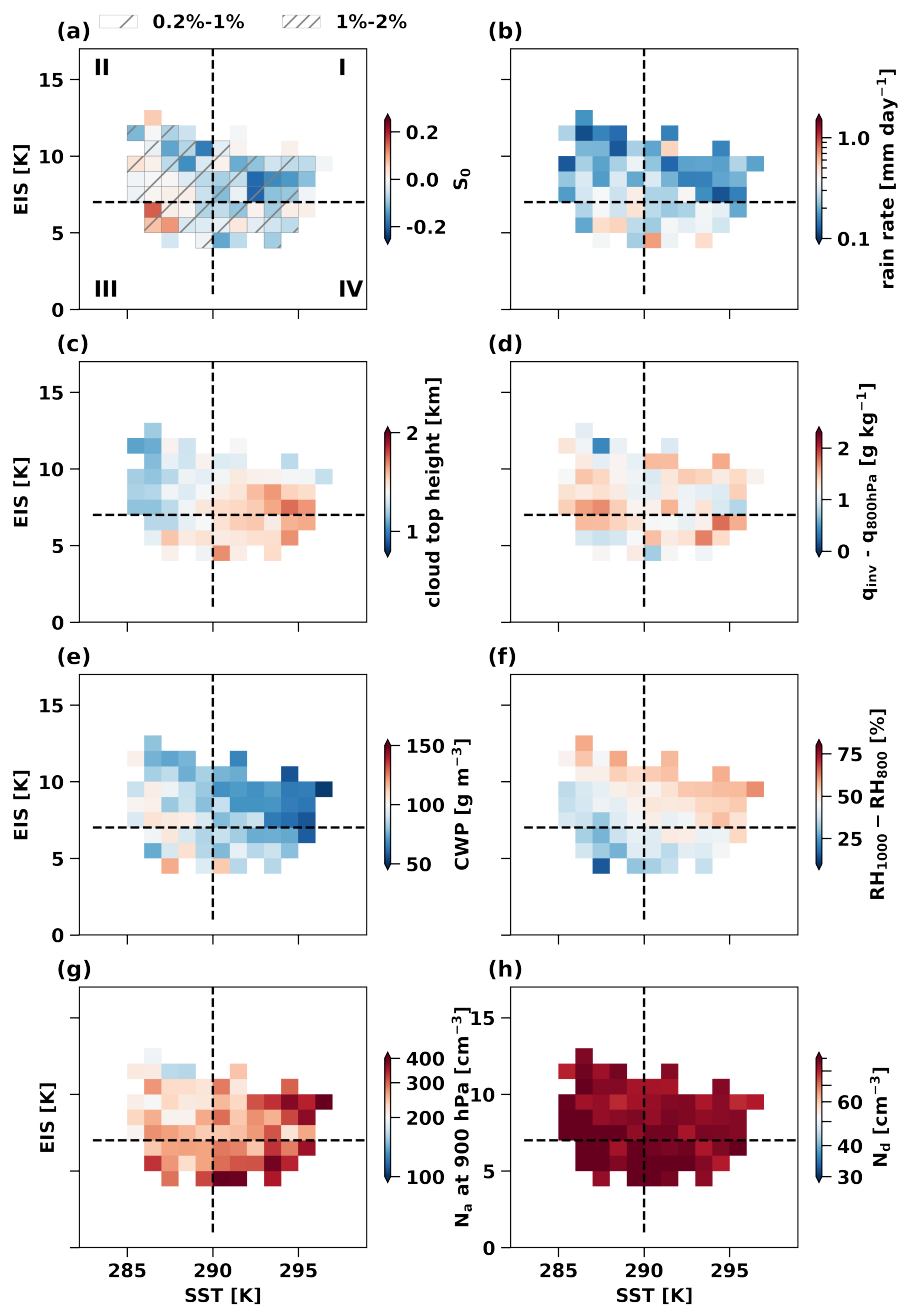


Figure S8. Same as Fig. 2 but for $N_d \geq 60\text{cm}^{-3}$.

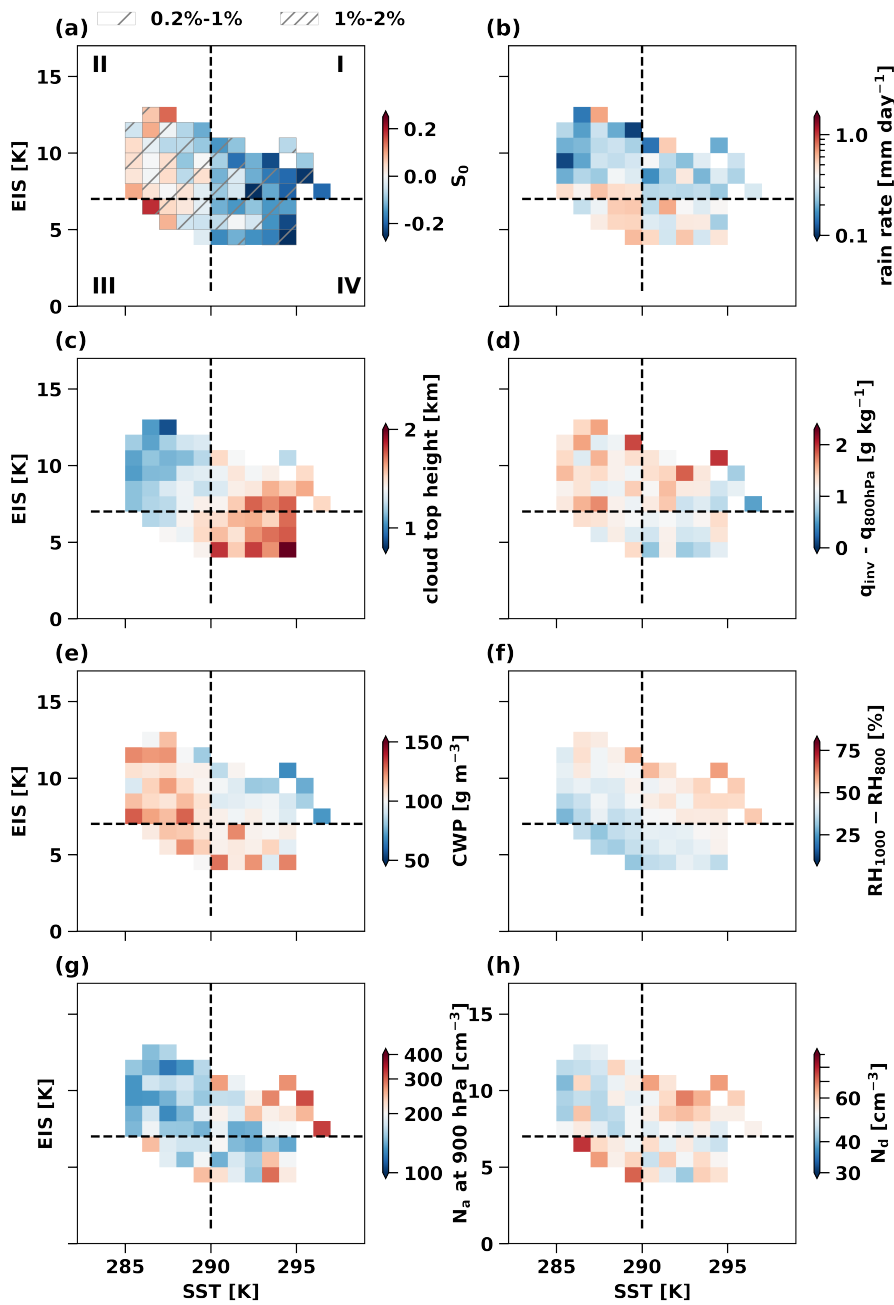


Figure S9. Same as Fig. 2 but for correlation coefficient between cloud albedo and cloud droplet number concentration greater than 0.5.